

---

# Neutrino Conversion and Neutrino Astrophysics\*

---

A. Yu. Smirnov

*International Center for Theoretical Physics, Strada Costiera 11,  
34100 Trieste, Italy and*

*Institute for Nuclear Research, RAN, Moscow, Russia*

---

## Abstract

We consider main ingredients which determine neutrino transformations in media. Strong transformations relevant for the astrophysics can be due to large depth oscillations, resonance conversion, parametric resonance effect, interplay of oscillations and inelastic collisions. Properties of transitions are discussed using the graphic representation. The applications of the transitions to supernova neutrinos are described. The supernova neutrinos can probe whole neutrino mass spectrum. Their studies will help to identify the pattern of neutrino mass and mixing.

## 1. Introduction

The effects of neutrino propagation are determined by the following three ingredients:

- (i) Properties of media (physical conditions): density, chemical composition, polarization, motion;
- (ii) Density profiles: effective density distribution on the way of neutrinos;
- (iii) Pattern of neutrino masses and mixing.

Variety of the physical conditions, profiles and possible mass spectra of neutrinos determines a large number of effects which can be observed by present and future experiments.

In this review we will consider the system of three (or more) neutrinos  $\nu_f = (\nu_e, \nu_\mu, \nu_\tau \dots)$  mixed by mass terms (vacuum mixing). In the ultrarelativistic limit a propagation of these neutrinos is described by the evolution equation [1, 2]

$$i \frac{d\nu_f}{dt} = H \nu_f, \quad H \simeq \frac{M^2}{2E} + V_f, \quad (1)$$

---

\* Talk given at the Symposium "New Era in Neutrino Physics", Tokyo Metropolitan University, Japan, 11-12 June, 1998.

where

$$M = SM^{diag}S^\dagger \quad (2)$$

is the mass matrix in flavor basis. Here  $M^{diag} \equiv diag(m_1, m_2, m_3, \dots)$ ,  $m_i$  are the masses of neutrinos.  $S$  is the mixing matrix determined by  $\nu_f = S\nu$ , where  $\nu = (\nu_1, \nu_2, \nu_3, \dots)$  are the eigenstates of the mass matrix.  $E$  is the neutrino energy.  $V_f$  is the matrix of the effective potentials which describes the interactions of neutrinos with medium. The real part of the potential corresponds to refraction effect. The imaginary part describes inelastic collisions which lead to depart of the neutrino from the coherent state. The ratio of the imaginary to real parts of the potentials is  $V_I/V_R \sim \sqrt{s}/m_W \ll 1$  for low energy neutrinos, and for many applications one can neglect  $V_I$ . The Hamiltonian is hermitian in this case.

For two neutrino case, *e.g.*  $(\nu_e, \nu_\mu)$ , we get explicitly:

$$H = \frac{\Delta m^2}{4E} \begin{pmatrix} -\cos 2\theta + 4V_{e\mu}E/\Delta m^2 & \sin 2\theta \\ \sin 2\theta & \cos 2\theta \end{pmatrix}, \quad (3)$$

where  $\theta$  is the mixing angle in vacuum,  $\Delta m^2 \equiv m_2^2 - m_1^2$ , and  $V_{e\mu} \equiv V_e - V_\mu$ .

## 2. Physical Conditions

Properties of medium are described by the effective potential  $V_f$  which can be calculated as

$$V_f = \langle \Psi | H_{int} | \Psi \rangle. \quad (4)$$

Here  $\Psi$  is the wave function of the system of neutrino and medium, and  $H_{int}$  is the Hamiltonian of interaction. According to the standard model the matrix of the potentials in the flavor basis,  $V_f$ , is practically diagonal:  $V_f = diag(V_e, V_\mu, V_\tau, 0\dots)$ . Only difference of the diagonal elements is important. The Hamiltonian  $H_{int}$  is the effective four fermion Hamiltonian due to exchange of the  $W$  and  $Z$  bosons:

$$H_{int} = \frac{G_F}{\sqrt{2}} \bar{\nu} \gamma^\mu (1 - \gamma_5) \nu \{ \bar{e} \gamma_\mu (g_V + g_A \gamma_5) e + \bar{p} \gamma_\mu (g_V^p + g_A^p \gamma_5) p + \bar{n} \gamma_\mu (g_V^n + g_A^n \gamma_5) n \}, \quad (5)$$

where  $G_F$  is the Fermi coupling constant;  $g_V$  and  $g_A$  are the vector and the axial vector coupling constants.

Let us consider the effect of scattering on electrons. We define the vector of polarization of electrons as

$$\vec{\lambda}_e \equiv \omega_e^\dagger \vec{\sigma} \omega_e, \quad (6)$$

where  $\omega_e$  is the two component spinor. Suppose electrons have some density distribution over the momentum,  $\vec{p}_e$  and polarization  $\vec{\lambda}_e$ :

$$\frac{f(\vec{\lambda}_e, \vec{p}_e)}{(2\pi)^3}.$$

Then the total number density of electrons,  $n_e$ , equals

$$n_e = \sum_{\vec{\lambda}} \int \frac{d^3 p_e}{(2\pi)^3} f(\vec{\lambda}_e, \vec{p}_e). \quad (7)$$

The average polarization of electrons is defined as

$$\langle \vec{\lambda}_e \rangle = \frac{1}{n_e} \sum_{\vec{\lambda}} \int \frac{d^3 p_e}{(2\pi)^3} \vec{\lambda} f(\vec{\lambda}_e, \vec{p}_e). \quad (8)$$

The matrix element (4) can be calculated as

$$\sum_{\vec{\lambda}} \int \frac{d^3 p_e}{(2\pi)^3} f(\vec{\lambda}_e, \vec{p}_e) \langle e_{p,\lambda} | \bar{e} \gamma_\mu (g_V + g_A \gamma_5) e | e_{p,\lambda} \rangle, \quad (9)$$

where for free electrons  $|e_{p,\lambda}\rangle$  is the solution of the Dirac equation.

Let us consider the results of calculations of the potentials for the most important cases (for recent discussion see [3]).

### 2.1. Unpolarized medium

In this case  $\vec{\lambda}_e = 0$ , the vector current only contributes to the potential:

$$V = V^V(\vec{p}_e) = \sqrt{2} G_F g_V \frac{f_e(\vec{p}_e)}{(2\pi)^3} \left( 1 - \frac{\vec{p}_e \cdot \hat{k}_\nu}{E_e} \right), \quad (10)$$

where  $\hat{k}_\nu \equiv \vec{p}_\nu / |\vec{p}_\nu|$  with  $\vec{p}_\nu$  being the neutrino momentum,  $E_e$  is the energy of electrons. For non-relativistic electrons (as well as for isotropic distribution of the ultrarelativistic electrons) only  $\gamma^0$  component of the vector current gives non-zero effect and its matrix element equals the density of electrons,  $n_e$ . Therefore the integration of (10) over  $\vec{p}$  leads to [1]

$$V = \sqrt{2} G_F n_e g_V. \quad (11)$$

In the case of moving medium also space components of the vector current give non-zero contribution:  $\langle \psi_e | \vec{\gamma} | \psi_e \rangle \propto \vec{v}$  and [4, 3]

$$V = \sqrt{2} G_F n_e g_V (1 - v \cdot \cos \beta), \quad (12)$$

where  $\beta$  is the angle between the momenta of the electrons and neutrino. In the case of isotropic distribution the second term in (12) disappears.

### 2.2. Polarized medium

Now the axial vector current,  $\vec{\gamma}\gamma_5$ , also gives the contribution which is proportional to the polarization of electrons [4, 3]. In the *non-relativistic* case we get

$$V^A \approx -\sqrt{2}G_F g_A n_e (\hat{k}_\nu \cdot \langle \vec{\lambda}_e \rangle), \quad (13)$$

where the average polarization of electrons is defined in (8). In the case of *ultra-relativistic electrons* we find

$$V^A \approx \sqrt{2}G_F g_A \frac{f(\vec{\lambda}_e, \vec{p}_e)}{(2\pi)^3} (\hat{k}_e \cdot \vec{\lambda}_e) \left[ 1 - (\hat{k}_e \cdot \hat{k}_\nu) \right]. \quad (14)$$

Here  $\hat{k}_e \equiv \vec{p}_e/|\vec{p}_e|$ . If electrons are polarized in the transverse plane the potential is zero for any momenta of neutrinos. The potential is suppressed if neutrinos and electrons are moving in the same direction.

Suppose, the two equal electron fluxes move in opposite directions but have the same polarization along the momentum. Such a configuration is realized in the *magnetized medium* (electrons in the lowest Landau level). For this case we find using (14):

$$V^A = -\sqrt{2}G_F g_A n_e (\hat{k}_\nu \cdot \vec{\lambda}_e). \quad (15)$$

Here  $n_e$  is the total concentration of electrons in both fluxes. Notice that this relativistic expression coincides with the non-relativistic formula (13).

The total effective potential resulting from neutrino scattering on electrons, protons and neutrons in an electrically neutral medium can be written in the form:

$$V = \sqrt{2}G_F n_e \left[ g_V - g_A \hat{k}_\nu \cdot \langle \vec{\lambda}_e \rangle \right] + \sqrt{2}G_F n_n g_V^n. \quad (16)$$

Here, the second term describes neutrino-nucleon scattering with  $n_n$  being the neutron concentration. Notice that in the electrically neutral medium the neutral current contributions from the neutrino-proton and the neutrino-electron scattering cancel each other and only neutrons contribute. Furthermore, in the case of unpolarized neutrons at rest, the zeroth component of vector current contributes to the potential only.

### 2.3. Difference of potentials

Effect of a medium on neutrino propagation is determined by the difference of potentials. For  $\nu_e \rightarrow \nu_\mu, \nu_\tau$  (flavor) conversion only the charge current neutrino-electron scattering gives a net contribution. Taking  $g_V = -g_A = 1$  one finds from (16)

$$V_{e\mu} = \sqrt{2}G_F n_e \left[ 1 + \hat{k}_\nu \cdot \langle \vec{\lambda}_e \rangle \right] = \sqrt{2}G_F n_e [1 + \langle \lambda_e \rangle \cos \alpha], \quad (17)$$

where  $\alpha$  is the angle between the neutrino momentum and the averaged polarization vector of electrons. There is no effect of nucleons in this case. Depending on the direction of polarization the axial term can either enhance or suppress the potential. The maximal effect is obtained in the case of complete polarization in the direction of the neutrino momentum,  $\langle \lambda_e \rangle = 1$ . In the case of complete polarization against the neutrino momentum,  $\cos \alpha = -1$ ,  $\langle \lambda_e \rangle = 1$ , we get  $V_{e\mu} = 0$ . Clearly, the axial vector term can not overcome the vector term,  $|V_V| \geq |V_A|$ .

In the case of conversion into sterile neutrinos, the difference of potentials gets also the contribution from the neutrino-nucleon scattering. If nucleons are unpolarized, we find for  $\nu_e - \nu_s$  system:

$$V_{es} = \sqrt{2}G_F n_e \left[ \left( 1 - \frac{n_n}{2n_e} \right) + \frac{1}{2} \hat{k}_\nu \cdot \langle \vec{\lambda}_e \rangle \right]. \quad (18)$$

Now the polarization term can be bigger than the vector current one, thus leading to the possibility of level crossing induced by the axial term. The latter may have some implication to the neutrinos in the central parts of supernova.

For the  $\nu_\mu - \nu_s$  system we get:

$$V_{\mu s} = \sqrt{2}G_F \left( -\frac{n_n}{2} - \frac{n_e}{2} \hat{k}_\nu \cdot \langle \vec{\lambda}_e \rangle \right). \quad (19)$$

This result can be applied to the atmospheric neutrinos.

#### 2.4. Magnetized Medium

In presence of the magnetic field the energy spectrum of electrons is quantized. It consists of the lowest Landau level,  $n = 0, \lambda_z = -1$ , plus pairs of degenerate levels with opposite polarizations. As a result, the contributions from all the levels but the lowest one cancel each other [5, 6, 7]. So, the average polarization of electrons is determined by  $n_0$  – the electron number density in the lowest Landau level:

$$\langle \lambda_e \rangle = -\frac{n_0}{n_e}. \quad (20)$$

In strongly degenerate electron gas

$$n_0 \approx \frac{eB p_F}{2\pi^2}, \quad (21)$$

where  $p_F = \sqrt{\mu^2 - m_e^2}$  is the Fermi momentum determined from the expression for the total electron concentration  $n_e$ . In the weak field limit,  $eB \ll p_F^2$ , we get the usual expression for  $p_F$  in a medium without magnetic field:  $p_F \simeq (3\pi^2 n_e)^{1/3}$ . Inserting this  $p_F$  in (21) we have

$$n_0 = \frac{eB}{2} \left( \frac{3n_e}{\pi^4} \right)^{1/3}. \quad (22)$$

Therefore  $\langle \lambda_e \rangle$  increases linearly with  $B$  and decreases as  $n_e^{-2/3}$ . Using (17) and (20) we get for the effective potential of the electrons [5, 8]

$$V = \sqrt{2}G_F n_e - \frac{G_F e B}{\sqrt{2}} \left( \frac{3n_e}{\pi^4} \right)^{1/3} \cos \alpha_B , \quad (23)$$

where  $\alpha_B$  is the angle between neutrino momentum and the magnetic field. The second term may be important in the central parts of supernovae [9].

### 2.5. Non-local corrections. Thermal medium

The motion of scatterers manifests also through the correction to the propagator of the vector boson:  $G_F \rightarrow G_F(1 + q_W^2/m_W^2)$ , where  $q_W^2$  is the four momentum of the intermediate boson squared. Consequently,

$$V \rightarrow V_0(1 + q_W^2/m_W^2).$$

In thermal bath  $q_W^2 \sim T^2$ , and one gets [10]

$$V_T \sim \sqrt{2}G_F n_e A \frac{T^2}{m_W^2} , \quad (24)$$

where  $A$  is the constant which depends on the composition of plasma. The crucial feature is that the thermal correction (24),  $V_T$ , has the same signs for neutrinos and antineutrinos. This comes about from the following facts: (i) For  $\nu e$ -scattering the  $W$  – exchange occurs in the  $t$  channel, whereas for  $\bar{\nu} e$ -scattering – in the  $s$  channel. Therefore  $q_W^2 < 0$  for neutrinos and  $q_W^2 > 0$  for antineutrinos. (ii) The currents of neutrinos and antineutrinos have opposite signs. So, in the transition from neutrino channel to antineutrino channel the amplitude changes the sign twice.

In thermal bath with non-zero lepton charge (the Early Universe) the potential can be written as

$$V = \sqrt{2}G_F n_\gamma \left( \Delta L + A \frac{T^2}{m_W^2} \right) , \quad (25)$$

where  $n_\gamma$  is the photon density,  $\Delta L = (n_L - n_{\bar{L}})/n_\gamma$  is the leptonic asymmetry and  $n_L, n_{\bar{L}}$  are the concentrations of the leptons and antileptons. In CP symmetric medium only thermal correction survives and  $V = V_0 A T^2/m_W^2$ .

In the Early Universe the matter effects can be important for oscillations into sterile neutrinos. Matter influences differently the neutrino and antineutrino channels, so that transitions  $\nu_\tau \rightarrow \nu_s$ , and  $\bar{\nu}_\tau \rightarrow \bar{\nu}_s$  can create the  $\nu_\tau - \bar{\nu}_\tau$  asymmetry in the Universe [11]. The leptonic asymmetry influences the primordial

nucleosynthesis. It can also suppress further the production of sterile neutrinos, so that the concentration of these neutrinos is much smaller than the equilibrium concentration even in the case of large mixing angle and large mass squared difference.

### 3. Density Profiles

When transitions of neutrinos are strong? This question is especially relevant for astrophysics, where the effects have observable consequences provided that transition probabilities are of the order one (apart from a few exceptional cases). Physical conditions are described by the effective potentials. The result of conversion depends on the density profile, that is, on the change of the effective potential on the way of neutrinos.

We start here with some elements of dynamics and then consider different profiles which lead to strong transitions.

#### 3.1. Elements of dynamics

Let us consider the evolution equation (1) for two neutrino species ( $\nu_e, \nu_\mu$ ). The Hamiltonian is the function of the electron density, and consequently, the time:  $H = H(n_e(t))$ . For a given moment of time  $t$  we can introduce the instantaneous eigenstates of  $H$ ,  $\nu_{im}(t)$ , and eigenvalues of  $H$ ,  $E_{im}(t)$ , ( $i = 1, 2$ ):

$$H(t)\nu_{im}(t) = E_{im}(t)\nu_{im}(t) .$$

The eigenstates are related to the flavor states as

$$\nu_f = S(\theta_m)\nu_H. \quad (26)$$

This equality can be considered as the definition of the mixing matrix in medium,  $S(\theta_m)$ , and the mixing angle in medium  $\theta_m$ . Both the mixing angle and the eigenvalues are functions of electron density:  $\theta_m = \theta_m(n_e)$ ,  $E_{im} = E_{im}(n_e)$ . For  $\theta_m$  we have explicitly

$$\tan 2\theta_m = \frac{\sin 2\theta}{\cos 2\theta - 2\sqrt{2}G_F n_e E / \Delta m^2} . \quad (27)$$

The mixing becomes maximal ( $\theta_m = \pi/4$ ) at the resonance density

$$n_e^R = \frac{\Delta m^2 \cos 2\theta}{2E \sqrt{2}G_F} . \quad (28)$$

From (26) we find the inverse relation:

$$\nu_{1m} = \cos \theta_m \nu_e - \sin \theta_m \nu_\mu, \quad \nu_{2m} = \cos \theta_m \nu_\mu - \sin \theta_m \nu_e. \quad (29)$$

According to (29) the mixing angle  $\theta_m$  determines the  $\nu_e$ -,  $\nu_\mu$ - (that is, flavor) content of the neutrino eigenstates. When  $n_e$  changes with distance,  $\theta_m$  also changes according to (27). Then from (29) we get the following conclusion. In the nonuniform medium the flavors of the eigenstates change: they uniquely follow a change of the electron density. When density changes from  $n_e \gg n_e^R$  to  $n_e \ll n_e^R$  (and if the vacuum mixing is small), the flavor of the  $\nu_{1m}$  changes from almost  $\nu_\mu$  to  $\nu_e$  and the flavor of  $\nu_{2m}$  – from  $\nu_e$  to  $\nu_\mu$  (fig. 1).

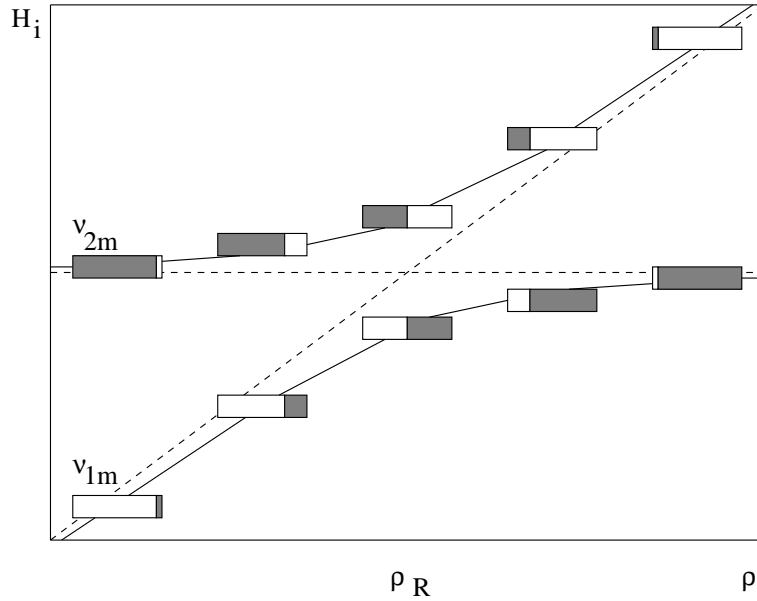


Fig. 1 Energies  $H_i$  (solid lines) and flavors of the neutrino eigenstates as functions of the effective density  $\rho \equiv m_N n_e$  ( $m_N$  is the mass of the nucleon). White parts of boxes represent the electron flavor and shadowed parts are the muon flavor.

### 3.2. Degrees of freedom

An arbitrary neutrino state can be expressed in terms of the instantaneous eigenstates as

$$\nu(t) = \cos \theta_a \nu_{1m} + \sin \theta_a \nu_{2m} e^{i\phi}, \quad (30)$$

where

- $\theta_a = \theta_a(t)$  determines the admixtures of the eigenstates in a given state;
- $\phi(t)$  is the phase difference between the two eigenstates (phase of oscillation).



tions):

$$\phi(t) = \int_0^t \Delta H dt' + \phi(t)_T, \quad (31)$$

where  $\Delta H \equiv H_1 - H_2$ , the integral determines the adiabatic phase and  $\phi(t)_T$  is the rest which can be related to violation of adiabaticity. It may also have a topological contribution (Berry phase) in more complicated systems;

- Flavor content of the eigenstates depends on time and changes according to mixing angle change  $\theta_m(n_e(t))$ , as we have discussed in sect. 3.1.

Different processes are associated with these three degrees of freedom.

### 3.3. Density matrix and Graphic representation

We will consider dynamics of transitions in different media using graphic representation [12]. The representation is based on analogy of the neutrino evolution with behaviour of spin of the electron in the magnetic field. Indeed, a neutrino state can be described by vector

$$\vec{\nu} = (\text{Re}\nu_e^\dagger\nu_\mu, \text{Im}\nu_e^\dagger\nu_\mu, \nu_e^\dagger\nu_e - 1/2), \quad (32)$$

where  $\nu_i$ , ( $i = \mu, e$ ) are the neutrino wave functions. (The elements of this vector are nothing but components of the density matrix.) Introducing another vector:

$$\vec{B} \equiv \frac{2\pi}{l_m}(\sin 2\theta_m, 0, \cos 2\theta_m) \quad (33)$$

( $l_m = 2\pi/\Delta H$  is the oscillation length in medium) which corresponds to the magnetic field, one gets from the evolution equations for the wave functions (1) the equation

$$\frac{d\vec{\nu}}{dt} = (\vec{B} \times \vec{\nu}). \quad (34)$$

The vector  $\vec{\nu}$  moves (see fig. 2) on the surface of the cone with axis  $\vec{B}$  according to increase of the oscillation phase,  $\phi$ . The direction of the axis,  $\vec{B}$ , is determined by  $2\theta_m$  (33). The cone angle – the angle between  $\vec{\nu}$  and  $\vec{B}$  – coincides with  $2\theta_a$  (see (30)). It depends both on mixing angle and on the initial state, and in general, changes in the process of evolution. If the initial state is  $\nu_e$ , the angle equals  $2\theta_a = 2\theta_m$  in the initial moment. The projection of  $\vec{\nu}$  on the axis  $\nu_z$ , gives the probability to find  $\nu_e$  in a state  $\vec{\nu}$ :

$$P \equiv \nu_e^\dagger\nu_e = \nu_z + \frac{1}{2} = \cos^2 \frac{\theta_z}{2}. \quad (35)$$

Here  $\nu_z \equiv 0.5 \cos \theta_z$ , and  $\theta_z$  is the angle between  $\vec{\nu}$  and the axis  $\nu_z$ .

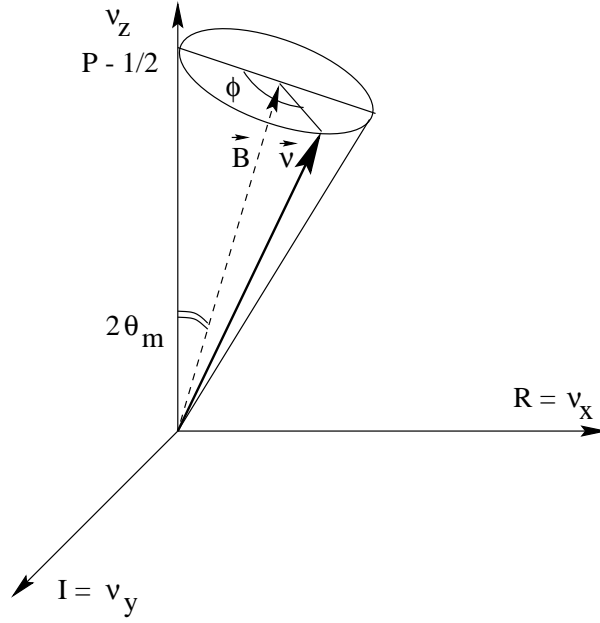


Fig. 2 Graphic representation of the neutrino oscillations in the uniform medium (see text).  $R \equiv \text{Re}\nu_e^\dagger\nu_\mu$ ,  $I \equiv \text{Im}\nu_e^\dagger\nu_\mu$ ,  $P \equiv \nu_e^\dagger\nu_e$ .

#### 3.4. Oscillations in the uniform medium

In medium with constant density ( $\theta_m = \text{const}$ ), the evolution consists of  $\vec{\nu}$ -precession around  $\vec{B}$ :  $\vec{\nu}$  moves monotonously according to increase of the oscillation phase,  $\phi$ . The evolution of neutrino has a character of oscillations. Oscillations are the consequence of the monotonous change of the phase. Only this degree of freedom operates. Flavors of the eigenstates and the admixtures of the eigenstates in a given state are fixed:

$$\theta_m = \text{const}, \quad \theta_a = \text{const}, \quad \phi = (H_2 - H_1)t. \quad (36)$$

The mixing angle depends on the neutrino energy. Therefore for different energies vectors of the neutrino states will rotate around different axes with different cone angles. At the resonance energy, the rotation proceeds around  $\nu_x$ , and the cone angle equals  $\pi/2$ .

Obviously, to get large transition effect one needs to have both large mixing angle and the phase of oscillations about  $\pi$ :  $\theta_m \sim \pi/4$ ,  $\phi \sim \pi$ . This condition can be realized inside the Earth, where the density profile can be approximated by several layers with constant densities.

### 3.5. Adiabatic resonance conversion

Suppose the density varies on the way of neutrinos (*e.g.* decreases) slowly. In this case the evolution is characterized by the following features:

1. Mixing angle changes according to density change. Correspondingly, flavors of the eigenstates change.
2. If  $n_e$  changes slowly enough, so that

$$|\dot{\theta}_m| \ll |H_2 - H_1|, \quad (37)$$

then in the first approximation the transitions  $\nu_{1m} \leftrightarrow \nu_{2m}$  can be neglected. The condition (57) is called the *adiabaticity condition*. In the adiabatic approximation (as in the cases of vacuum and uniform medium) the eigenstates propagate independently. This means that the angle  $\theta_a$  is constant; admixtures of the eigenstates are conserved.

3. The phase between the eigenstates changes, leading to oscillations.

Thus, the evolution in the adiabatic approximation is characterized by

$$\theta_m = \theta_m(n_e), \quad \theta_a = const, \quad \phi = \int (H_2 - H_1) dt. \quad (38)$$

The interplay takes place between the oscillations and the effects related to the change of flavors of the eigenstates. Graphically, the adiabatic conversion

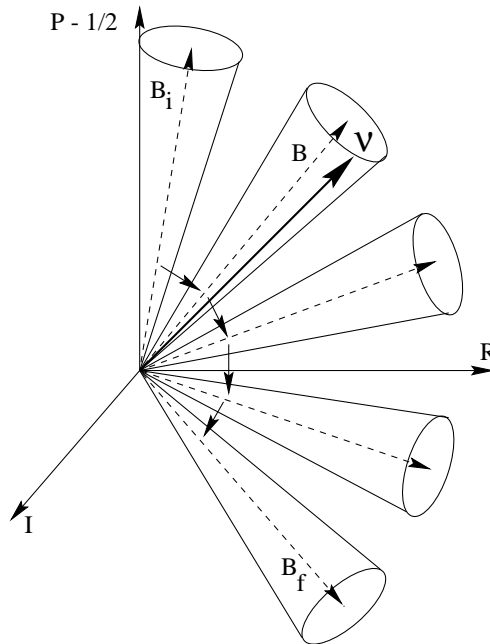


Fig. 3 Graphic representation of the neutrino adiabatic conversion (see text).

is described in the following way (fig. 3). The axis of the cone rotates according

to density change. The cone angle is unchanged (adiabaticity). The evolution consists of the rotation of the cone and the rotation of the neutrino vector on the surface of the cone.

A strong transition occurs when the interval of density changes is sufficiently large. The initial density should be larger than the resonance density, whereas the final density should be smaller than  $n_R$ .

### 3.6. Non-adiabatic resonance conversion

Let us consider again a medium with monotonously changed density. If the density changes rapidly, the adiabaticity condition turns out to be broken and the transitions  $\nu_{1m} \leftrightarrow \nu_{2m}$  become essential. This means that the admixtures of the eigenstates in a given state are changed, or equivalently, the angle  $\theta_a$  is no more a constant. In this case all three degrees of freedom operate:

$$\theta_m = \theta_m(n_e) , \quad \theta_a = \theta_a(t), \quad \phi = \int (H_2 - H_1) dt. \quad (39)$$

In the graphic representation (fig. 4) the axis of the cone rotates according to density change. The cone angle changes (violation of the adiabaticity). The neutrino vector moves on the surface of the cone (phase change). Typically,

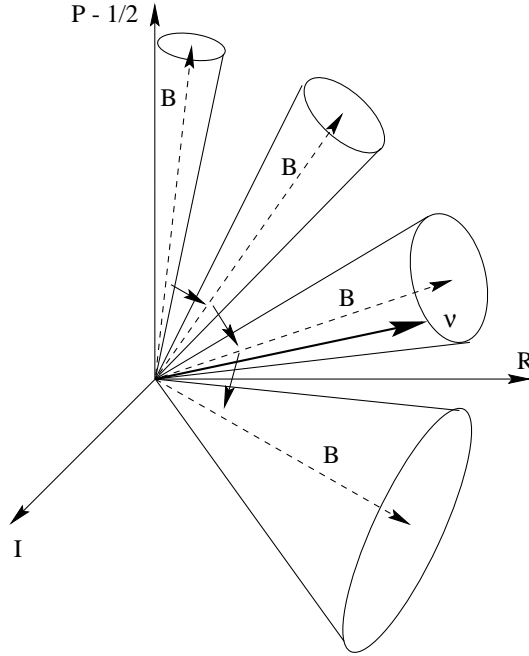


Fig. 4 Graphic representation of the non-adiabatic neutrino conversion (see text).

adiabaticity breaking leads to weakening of the flavor transition. Both adiabatic and non-adiabatic transitions can be realized inside the Sun and supernovae.

### 3.7. Conversion due to the parametric resonance

Strong transitions discussed in sect 3.4 - 3.6 imply an existence of the large effective mixing in whole medium (constant density) or at least in some layer (the resonance conversion). There is the way to get large transition without large (vacuum or even matter) mixing. This can be done with periodically changed density [13, 14].

The simplest example is the so called “castle wall” profile [14], when the period  $l_f$  is divided into two parts  $l_1$  and  $l_2$  ( $l_1 + l_2 = l_f$ ) and the density takes two different values  $n_1$  and  $n_2$  in parts  $l_1$  and  $l_2$  respectively (in general  $l_1 \neq l_2$ ).

General condition of the parametric resonance is that the effective oscillation length equals the period of density perturbation, or [15]

$$\int_{l_f} \frac{dx}{l_m} = k, \quad (k = 1, 2, 3, \dots). \quad (40)$$

For the “castle wall” profile the parametric resonance condition is reduced to equality of the oscillation phases acquired by neutrinos on the two parts of periods [16]:

$$\Phi_1 = \Phi_2 = \pi. \quad (41)$$

(The size of the layer equals half of the oscillation length in this layer.) Graphic representation is shown in fig. 5. Two different densities determine two positions of axes:  $\vec{B}_i = \vec{B}(2\theta_i)$  ( $i = 1, 2$ ). The angle between these axes,  $\Delta\theta \equiv 2\theta_1 - 2\theta_2$ , so called the “swing” angle, plays a key role in the enhancement mechanism. Let us consider an evolution of the neutrino for which the resonance condition (41) is fulfilled. Suppose,  $2\theta_1 > 2\theta_2$ , and the neutrino first propagate in the layer 1. This corresponds to  $\vec{\nu}$  precession around  $\vec{B}_1 = \vec{B}(2\theta_1)$ . At the border between the first and second layers the neutrino vector is in position  $\vec{\nu}(2)$  (which corresponds to phase acquired in the first layer,  $\Phi_1 = \pi$ ). At this moment the mixing angle changes suddenly:  $\theta_1 \rightarrow \theta_2$ . In the second layer  $\vec{\nu}$  precesses around new position of axis,  $\vec{B}_2 \equiv \vec{B}(2\theta_2)$ . Thus after one period the neutrino turns out in a position (3) and the cone angle increases as:  $\theta_a = 2\theta_1 + \Delta\theta$ . Further, the cone angle will continue to increase after each period by the double swing angle  $2\Delta\theta$ . The cone first opens and then shrinks in the opposite direction (see fig. 5).

The enhancement depends on number of periods (perturbations) and on the amplitude of perturbation which determines the swing angle. For small perturbations, large transition probability can be achieved after many periods. For sufficiently large “swing” angle even small number of periods is enough.

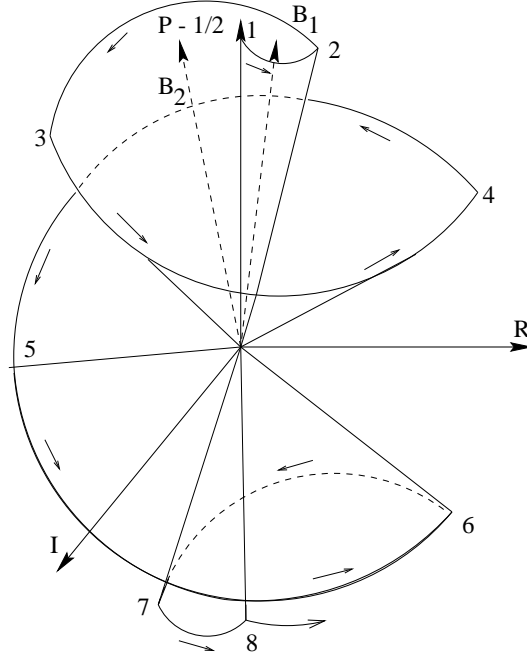


Fig. 5 Graphic representation of the parametric enhancement effect.

This mechanism can be realized inside the Earth [16, 17, 18, 19], where the perturbation is large  $\Delta\theta \sim 1$ , and strong effect is achieved even after “1.5 periods”.

### 3.8. Oscillations and inelastic collisions

Another example of significant ( $\sim O(1)$ ) transition without large mixing angle is when the oscillations are accompanied by the lost of coherence due to the inelastic collisions. At low energies the refraction length  $l_0$  can be much smaller than the absorption length  $l_{ab}$ :  $l_0 \ll l_{ab}$ . The oscillation length (being of the order  $l_0$ ) is also much smaller than  $l_{ab}$ . In this case one can consider the oscillations between two successive inelastic collisions. Since the time between two collisions fluctuate, one gets averaged oscillation effect which is characterized by  $0.5 \sin^2 2\theta_m$ . Collision splits a neutrino state into pure flavor components and further oscillations of these components will be independent. The process has a statistical character and the probability converges to 1/2, independently on mixing angle. The system approaches the “equilibrium”.

Graphically the effect of absorption and inelastic scattering (a depart from the coherence) is equivalent to shrinking the neutrino vector (and the cone).

### 3.9. Non-adiabatic perturbations

Small density perturbation can lead to strong “inverse” effect: The adiabatic transition results in almost complete transformation of one neutrino species into another one. Suppose that the density profile has some small perturbation  $\Delta n$  which breaks adiabaticity. If a size of the perturbation is comparable with the size of the resonance layer:

$$\frac{\Delta n}{n} \sim \sin 2\theta , \quad (42)$$

the perturbation will induce transition with  $P \sim 1$  to the original neutrino flavor in certain energy range [20].

## 4. Dynamics in the multilevel system

Dynamics of transitions in a system of three (or more) neutrino species is, of course, much more complicated than in the  $2\nu$ - case. New effects appear, *e.g.*, CP-violation. In certain realistic situations ( mass hierarchy, smallness of mixing) the task can be reduced to the evolution in two neutrino systems. There are also some generic  $3\nu$ - effects which exist even in the case of mass hierarchy.

Let us consider the neutrino mass spectrum with:

$$\Delta m_{12}^2 \ll \Delta m_{23}^2 \approx \Delta m_{13}^2 . \quad (43)$$

The dynamics of propagation can be reduced to the  $2\nu$ - case in the following circumstances.

### 4.1. Short range experiment. Freeze out of subsystem.

Suppose the source - detector distance  $d$  is much smaller than the oscillation length associated with smallest mass splitting:

$$d \ll l_\nu = \frac{4\pi E}{\Delta m_{12}^2} . \quad (44)$$

In this case the phase difference between  $\nu_1$  and  $\nu_2$  acquired on the way  $d$  will be very small:  $\phi_{12} = 2\pi d/l_\nu \ll 1$ , which means that there is no evolution in the subsystem  $\nu_1 - \nu_2$ . This subsystem is “frozen”.

Let us consider, for instance, the decomposition of the  $\nu_e$ :

$$\nu_e = U_{e1}\nu_1 + U_{e2}\nu_2 + U_{e3}\nu_3 . \quad (45)$$

Since the internal evolution in the  $\nu_1 - \nu_2$  subsystem is frozen, we can consider this subsystem as the unique state

$$\tilde{\nu} \equiv \cos \theta_{12}\nu_1 + \sin \theta_{12}\nu_2 , \quad (46)$$

where

$$\cos \theta_{12} = \frac{U_{e2}}{\sqrt{U_{e1}^2 + U_{e2}^2}} \equiv \frac{U_{e2}}{\sqrt{1 - U_{e3}^2}} . \quad (47)$$

Now  $\nu_e$  state can be rewritten as

$$\nu_e = \sqrt{1 - U_{e3}^2} \tilde{\nu} + U_{e3} \nu_3 , \quad (48)$$

and the task is reduced to evolution of the  $2\nu$ - system  $\tilde{\nu} - \nu_3$  with the effective mixing parameter  $\sin \theta = U_{e3}$  and  $\Delta m^2 = m_3^2$ . This is the so called one level dominating scheme, when the oscillations are determined by flavor composition and the mass of the heaviest state  $\nu_3$  [21].

#### 4.2. Long range experiments. Decoupling of one state.

Let us consider the case when the source-detector distance is much larger than the oscillation length associated with the largest mass splitting:

$$d \gg l_\nu = \frac{4\pi E}{\Delta m_{23}^2} . \quad (49)$$

Oscillations due to  $\Delta m_{23}^2$  are usually averaged out or/and the coherence of the  $\nu_3$  with the rest of system is lost. The state  $\nu_3$  decouples, leading to the averaged oscillation result. Nontrivial evolution will be in the  $\nu_1 - \nu_2$  subsystem. Let us consider again the propagation of the  $\nu_e$  (45). Taking into account decoupling of the  $\nu_3$  we can write immediately the survival probability as [22]

$$P = (1 - U_{e3}^2)^2 P(\Delta m_{12}^2, \theta) + U_{e3}^4 . \quad (50)$$

Here  $P(\Delta m_{12}^2, \theta)$  is the survival probability in  $\tilde{\nu} \leftrightarrow \tilde{\nu}'$  transition, where  $\tilde{\nu}' = \cos \theta_{12} \nu_2 - \sin \theta_{12} \nu_1$  is the state orthogonal to  $\tilde{\nu}$ .

Notice that for solar neutrinos both regimes can be realized if  $\Delta m_{12}^2 \sim 10^{-10} \text{ eV}^2$  and  $\Delta m_{13}^2 \sim 10^{-5} \text{ eV}^2$ . Indeed, on the way from the center of the sun to its surface the  $\nu_1 - \nu_2$  subsystem is frozen, whereas on the way from the surface of the Sun to the Earth the state  $\nu_3$  decouples.

#### 4.3. Generic $3\nu$ -effect

In matter in the  $3\nu$ -case, the subsystem  $\nu_1 - \nu_2$  can give significant oscillation effect even for very small vacuum splitting  $\Delta m_{12}^2$  [23, 24, 25]. Indeed, matter gives the contribution to the level splitting,  $\Delta H \approx V$ , which dominates in the case  $\Delta m_{12}^2/2E \ll V$ . Therefore even for small  $\Delta m_{12}^2$ , the splitting, and consequently, the phase of oscillations can be large. However, the oscillation effect will be still strongly suppressed in the  $2\nu$ -case since with increase of splitting the effective



mixing decreases:  $\theta_m \propto \Delta m_{12}^2/2EV$ . As the consequence, the oscillations will have very small depth.

Such a situation can be avoided in schemes with three neutrino mixing and significant admixture of  $\nu_e$  in the heaviest state  $\nu_3$ . Suppose the potential satisfies inequality:

$$\frac{m_2^2}{2E} \ll V \ll \frac{m_3^2}{2E}. \quad (51)$$

The key point is that at this condition the matter does not change practically the flavors of the  $\nu_3$ . In particular, the admixture of  $\nu_e$ ,  $U_{e3}$ , will be unsuppressed. At the same time matter changes strongly flavors of two other eigenstates.

Let us consider the  $\nu_\mu \leftrightarrow \nu_\tau$  oscillations due to mixing of two lightest eigenstates 1 - 2 with splitting  $\Delta H_{12} \approx V$ . The mixing of these eigenstates would be absent, if  $\nu_{2m}$  had pure electron neutrino flavor. This occurs in the  $2\nu$  scheme. However, in the  $3\nu$ -case, a part of the  $\nu_e$ -flavor is in  $\nu_3$ . Therefore due to unitarity the admixture of  $\nu_e$  in  $\nu_{2m}$  should be smaller than 1:

$$U_{e2}^m = \sqrt{1 - U_{e3}^2} < 1, \quad (52)$$

and correspondingly, the admixtures of  $\nu_\mu$  and  $\nu_\tau$  flavors in  $\nu_{2m}$  should not vanish. As a consequence, light states are mixed and the  $\nu_\mu \leftrightarrow \nu_\tau$  oscillations exist with unsuppressed depth. It is easy to find flavors of the neutrino eigenstates in medium  $U_{fi}^m$  at the conditions (51):

$$\begin{aligned} U_{\mu 2}^m &= (U_{e2}^m)^{-1} U_{e3} U_{\mu 3}, & U_{\tau 2}^m &= (U_{e2}^m)^{-1} U_{e3} U_{\tau 3}, \\ U_{\mu 1}^m &= (U_{e2}^m)^{-1} U_{\tau 3}, & U_{\tau 1}^m &= (U_{e2}^m)^{-1} U_{\mu 3}. \end{aligned} \quad (53)$$

From here we get the depth of  $\nu_\mu \leftrightarrow \nu_\tau$  oscillations

$$4U_{\mu 1}^m U_{\tau 1}^m U_{\mu 2}^m U_{\tau 2}^m = \frac{4U_{e3}^2 U_{\mu 3}^2 U_{\tau 3}^2}{(1 - U_{e3}^2)^2} \quad (54)$$

which does not depend on matter density. Clearly, the oscillations disappear if  $U_{e3} = 0$ . Such an effect can be relevant for the atmospheric neutrinos.

## 5. Neutrino spectra and Neutrino Transitions

Let us consider phenomenology of different neutrino mass schemes. We will assume that all neutrino masses are below a few eV, so that both cosmological and structure formation bounds are satisfied without neutrino decay. We will concentrate on applications of the neutrino transitions considered in sect. 3 to supernova neutrinos [26, 27].

In supernova the density changes on the way of neutrinos from nuclear values to practically zero. With a such profile one can probe whole mass spectrum of neutrinos. Indeed, the resonance density can be estimated as

$$\rho_R \sim 10^6 \text{g/cm}^3 \frac{\Delta m^2}{1 \text{eV}^2}. \quad (55)$$

Since  $\Delta m^2 \leq m^2 < \text{few eV}^2$ , all the transitions (with one possible exception) will occur far outside the core which means that they do not influence collapse. The transitions can, however, influence the nucleosynthesis in the internal parts of star [28]

$$\rho_{NS} = (10^6 - 10^{10}) \text{g/cm}^3. \quad (56)$$

The transitions change properties of fluxes observed at the Earth. They occur in the resonance layers as well as on the way from the star to the Earth. The efficiency of transition in a given resonance is determined by the adiabaticity. The edge of the adiabatic domain in the  $(\Delta m^2 - \sin^2 2\theta)$ - plot can be described roughly by

$$\sin^2 2\theta > 10^{-5} \left( \frac{\Delta m^2}{1 \text{eV}^2} \right)^{-3/4}, \quad (57)$$

where  $\theta$  is the vacuum mixing angle of the resonating states. In the adiabatic domain the survival probability equals  $P_{\alpha-\alpha} \approx \sin^2 \theta$ .

Since  $\nu_\mu$  and  $\nu_\tau$  have identical production and detection properties, we can consider phenomenology in terms of any combinations of these states. We will denote these neutrinos as the non-electron,  $\nu_{ne}$ , neutrinos.

### 5.1. Effects of neutrino conversion

The neutrino transformations in supernovae lead to the following effects.

1. Disappearance of the neutronization peak. In the case of strong  $\nu_e \rightarrow \nu_s$  conversion the peak will not be observable both in the charged and in the neutral current interactions.
2. Change of flavor of the neutronization peak. The oscillations/conversion  $\nu_e \rightarrow \nu_{ne}$ , where  $\nu_{ne} \equiv \nu_\mu, \nu_\tau$ , lead to appearance of the  $\nu_{ne}$ -neutronization peak. This effect can be detected by comparison of signals in the charged current (sensitive to  $\nu_e$  only) and neutral current (sensitive to whole flux) interactions.
3. Modification of spectrum of the electron neutrinos during cooling stage. The  $\nu_e$ -spectrum at the Earth is

$$F_e(E) = F_e^0(E)P_{e \rightarrow e}(E) + F_x^0(E)P_{x \rightarrow e}(E), \quad (58)$$

where  $F_e^0$  and  $F_x^0$  are the original spectra of the electron neutrinos and non-electron ( $\nu_\mu, \nu_\tau$ ) neutrinos respectively.  $F_e^0$  is the soft and  $F_x^0$  is the hard component: the average energies of spectra satisfy inequality  $E(\nu_e) < E(\nu_x)$  and the difference follows from the difference of interactions of these neutrinos.  $P_{e \rightarrow e}$  and  $P_{x \rightarrow e}$  are the conversion probabilities which may not be related in the multilevel system:  $P_{x \rightarrow e} \neq 1 - P_{e \rightarrow e}$ .

If  $P_{e \rightarrow e} \approx 0$  and  $P_{x \rightarrow e} \approx 1$ , there is a complete interchange of the spectra. For the energy independent probabilities in the  $2\nu$ - case the effects can be characterized by “permutation” parameter [29]:  $p \equiv P_{x \rightarrow e}$ ,  $P_{e \rightarrow e} \equiv 1 - p$ . Complete interchange of spectra corresponds to  $p = 1$ . For  $p < 1$  (partial permutation),  $F_e(E)$  will have both soft and hard components.

If  $P$  depends on energy the distortion of the spectrum can be more complicated.

4. Modification of the  $\bar{\nu}_e$  spectrum. It can be described in a similar way.

Notice that transition effects in the neutrino and antineutrino channels are usually different. The resonance transitions (due to mass) in the neutrino channels are not accompanied by the transitions in the antineutrino channels.

Depending on the level crossing scheme one predicts different combinations of the above effects. In what follows we will consider predictions from different schemes and discuss the possibility to identify the scheme [30].

### 5.2. $3\nu$ scheme for solar and atmospheric neutrinos

Let us consider the hierarchical mass spectrum with

$$m_3 = (0.3 - 1) \cdot 10^{-1} \text{eV}, \quad m_2 = (2 - 4) \cdot 10^{-3} \text{eV}, \quad m_1 \ll m_2 \quad (59)$$

(see fig. 6).  $\nu_\mu$  and  $\nu_\tau$  mix strongly in  $\nu_2$  and  $\nu_3$ . The electron flavor is weakly mixed: it is mainly in  $\nu_1$  with small admixtures in the heavy states. Such a scheme has the following properties:

- (i) It explains the solar neutrino data via  $\nu_e \rightarrow \nu_2$  resonance conversion inside the Sun. Notice that  $\nu_e$  converts to  $\nu_\mu$  and  $\nu_\tau$  in comparable portions.
- (ii) The atmospheric neutrino anomaly is solved via  $\nu_\mu \leftrightarrow \nu_\tau$  oscillations. Small  $\nu_e$  admixture in  $\nu_3$  can lead to resonantly enhanced oscillations in matter of the Earth.
- (iii) There is no explanation of the LSND result, and the contribution to the Hot Dark Matter component of the universe is small:  $\Omega_\nu < 0.01$ .

The scheme can be probed by the long baseline experiments.

It is convenient to consider neutrino transitions in the basis  $\nu_e, \nu'_2, \nu'_3$ , where  $\nu'_2$  and  $\nu'_3$  diagonalize the mass matrix for  $\nu_\mu - \nu_\tau$  subsystem. The mixing of  $\nu_e$  with  $\nu'_2$  and  $\nu'_3$  is small: Since  $\nu'_2$  and  $\nu'_3$  coincide up to small corrections

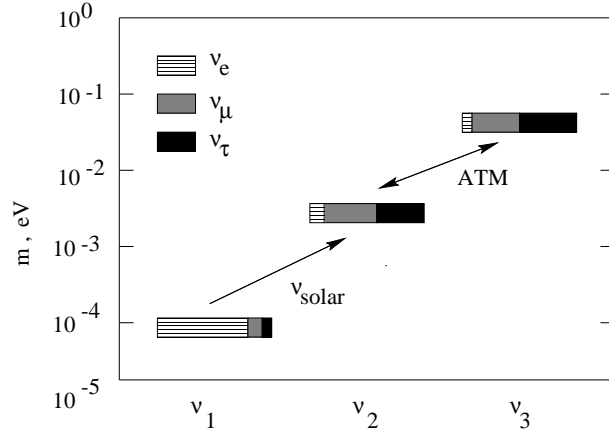


Fig. 6 Neutrino mass and mixing pattern of the scheme for the solar and atmospheric neutrinos. The boxes correspond to the mass eigenstates. The sizes of different regions in the boxes show admixtures of different flavors. Weakly hatched regions correspond to the electron flavor, strongly hatched regions depict the muon flavor, black regions present the tau flavor.

with mass eigenstates this mixing is determined by  $U_{ei}$ ,  $i = 2, 3$ .  $U_{e2}$  is fixed by the solar neutrino data, and  $U_{e3}$  is weakly restricted by the atmospheric neutrino results and reactor bounds.

In fig. 7 we show the level crossing scheme: the dependence of the eigenvalues on the density of medium. If  $U_{e2}$  is large enough, then all the level crossings are adiabatic, and the following transitions occur in a supernova:

$$\nu_e \rightarrow \nu'_3, \quad \nu'_3 \rightarrow \nu'_2, \quad \nu'_2 \rightarrow \nu_e. \quad (60)$$

All these transitions will occur in the outer layers of the stars, and therefore they do not influence collapse and nucleosynthesis. The transitions, however, modify fluxes expected at the Earth. The neutronization  $\nu_e$  peak disappears. Instead one would expect  $\nu_\mu/\nu_\tau$  neutronization peak which can be detected by the neutral current interactions. The  $\nu_e$  from cooling stage will have the hard spectrum  $F_x^0$ , the spectrum of non-electron neutrinos,  $\nu_\mu$  and  $\nu_\tau$ , will contain both the soft (original  $\nu_e$ ) and the hard components. The antineutrino signal is unchanged. Similar modifications are expected if one (among two) resonance crossings is non-adiabatic.

The modification of the scheme is possible in which all three neutrinos have approximately the same mass  $m_0$  (almost degenerate) but with  $\Delta m^2$  and mixings as before. In this case neutrinos give a significant ( $\Omega_\nu \sim 0.1$ ) contribution to the HDM. Since the  $\nu_e$  dominates in one of the mass eigenstates, the effective Majorana mass relevant for the neutrinoless double beta decay is about  $m_0$  and

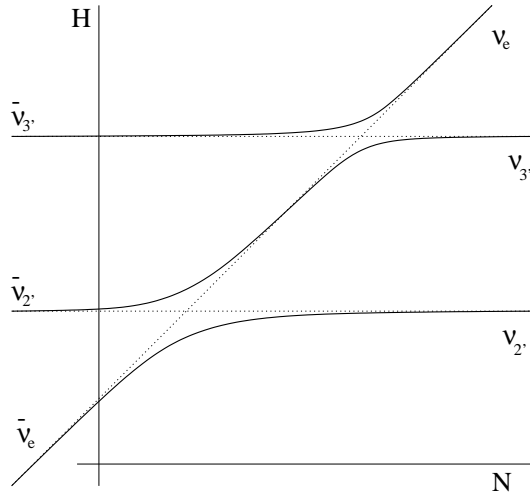


Fig. 7 The level crossing pattern of the scheme for the solar and atmospheric neutrinos. Solid lines show the eigenvalues of the system as functions of the density. The dashed lines correspond to energies of  $\nu_e$ ,  $\nu'_2$ , and  $\nu'_3$ . The part of the plot with  $N < 0$  corresponds to the antineutrino channels.

searches of the  $\beta\beta_{0\nu}$  decay give crucial check of this version [31].

### 5.3. Bi-maximal and bi-large mixings

The SK data on atmospheric neutrinos give strong evidence that mixing in the  $\nu_\mu - \nu_\tau$  channel is large (or even maximal). Probably mixing is large in other channels. In this context several schemes were elaborated [32].

In the bi-maximal scheme neutrinos have masses

$$m_3 = (0.3 - 3) \cdot 10^{-1} \text{eV}, \quad m_2 \sim 10^{-5} \text{eV}, \quad m_1 \ll m_2 \quad (61)$$

(see fig. 8).  $\nu_\mu$  and  $\nu_\tau$  mix maximally in  $\nu_3 = (\nu_\mu + \nu_\tau)/\sqrt{2}$ . The orthogonal combination,  $\nu'_2 \equiv (\nu_\mu - \nu_\tau)/\sqrt{2}$  strongly mixes with  $\nu_e$  in  $\nu_1$  and  $\nu_2$ . There is no admixture of  $\nu_e$  in the  $\nu_3$ . In this scheme

- (i) The solar neutrino problem can be solved via  $\nu_e \leftrightarrow \nu'_2$  “Just-so” vacuum oscillations. Notice that  $\nu_e$  converts equally to  $\nu_\mu$  and  $\nu_\tau$ .
- (ii) The atmospheric neutrino anomaly is solved via  $\nu_\mu \leftrightarrow \nu_\tau$  maximal depth oscillations.

The spectrum can supply significant amount of the HDM if all three neutrinos are strongly degenerate.

In fig. 9 we show the level crossing scheme of the spectrum in general case when there is small admixture of the  $\nu_e$  state in  $\nu_3$ . This can be checked by searches for an excess of the e-like events in the atmospheric neutrinos. In the

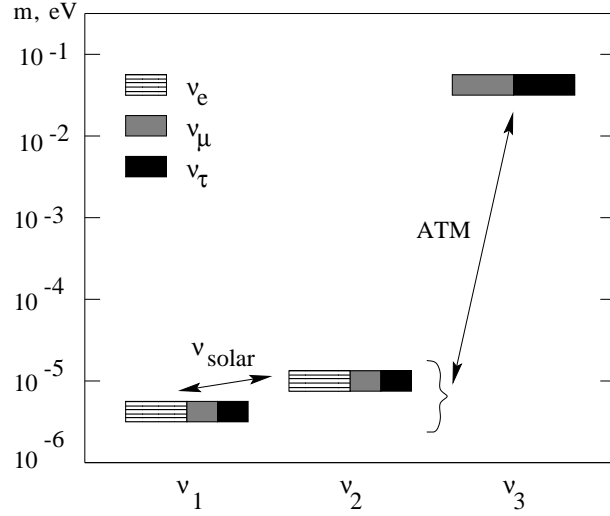


Fig. 8 The neutrino mass and mixing pattern of the bi-maximal mixing scheme.

strict bi-maximal mixing case, when  $U_{e3} = 0$ , the state  $\nu_3$  decouples and  $\nu_e$  mixes maximally with  $\nu'_2$ .

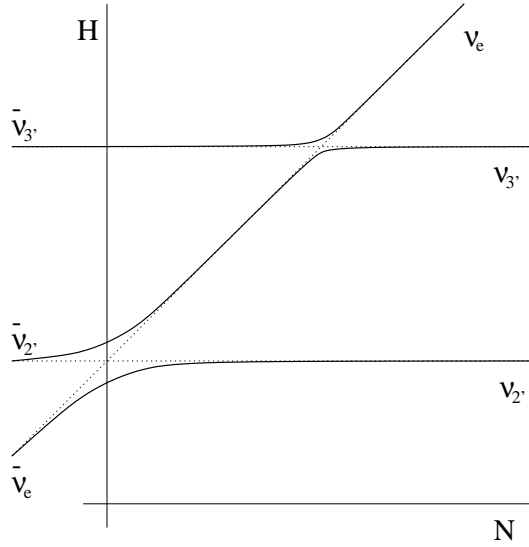


Fig. 9 The level crossing pattern of the bi-maximal mixing scheme with small admixture of the  $\nu_e$  in the heavy state.

For supernova neutrinos we predict the following. The electron neutrinos oscillate into combination of  $\nu_\mu$  and  $\nu_\tau$ , with maximal depth on the way from collapsing star to the Earth. Similarly, the electron antineutrinos oscillate into  $\bar{\nu}_\mu$  and  $\bar{\nu}_\tau$ . As the result the neutronization peak will consist of equal number of the electron and non-electron neutrinos (which could be checked by comparison

of signals due to the neutral and charged currents).

Also the spectra from the cooling stage will be modified. In particular, the  $\bar{\nu}_e$ -spectrum will have both the soft (original  $\nu_e$ ) component and the hard component (original  $\nu_\mu$ ) in equal portions: the permutation parameter is 0.5. The same holds for  $\nu_e$ .

Situation can be different, if there is some admixture of the  $\nu_e$  in  $\nu_3$ . Now the  $\nu_e - \nu'_3$  level crossing occurs (fig. 9), and if the adiabaticity condition is fulfilled one expects:

$$\nu_e \rightarrow \nu'_3, \quad \nu'_3 \rightarrow \nu'_2, \quad \nu'_2 \rightarrow \nu_1. \quad (62)$$

Recall that  $\nu_1$  is the maximal mixture of the electron and non-electron neutrinos. Therefore one expects: (i) complete (in contrast with previous case) disappearance of the  $\nu_e$  neutronization peak and appearance of the peak of non-electron neutrinos; (ii) the electron neutrinos with the hard spectrum (of original  $\nu_\mu$ ); (iii) muon and tau neutrinos with both the soft and the hard components. (iv) At the same time  $\bar{\nu}_e$  will have composite spectrum with hard and soft components. This distinguishes bi-maximal scheme from that of sect. 5.2.

The mixing of  $\nu_e$  can be non-maximal but large. If then  $m_2 \sim (3-4) \times 10^{-3}$  eV, the solar neutrino deficit can be explained by the large mixing angle MSW solution. The consequences for supernova neutrinos are rather similar to previous case. At the same time the permutation parameter for  $\bar{\nu}_e$  can be smaller. That is, the contribution of the hard component to  $\bar{\nu}_e$  spectrum is smaller.

One can introduce a degeneracy of neutrinos (keeping the same  $\Delta m^2$ ) to get significant amount the HDM in the Universe. Now the effective Majorana mass of the electron neutrino can be small due to cancellation related to large mixing.

Let us comment on the version of the bi-maximal scheme with inverted mass hierarchy:  $m_1 \approx m_2 \gg m_3$ , when two states with maximal (or large)  $\nu_e$  mixing are heavy and degenerate, whereas the third state with large  $\nu_\mu - \nu_\tau$  mixing and small  $\nu_e$  admixture is light. In this scheme the  $\nu_e - \nu'_3$  level crossing occurs in the *antineutrino* semiplane, so that in the supernova  $\bar{\nu}_e$  will be strongly converted into combination of  $\bar{\nu}_\mu - \bar{\nu}_\tau$  and vice versa. As the result the  $\bar{\nu}_e$ 's will have hard spectrum.

#### 5.4. Models with sterile neutrinos

There are two motivations for the introduction of sterile neutrinos: (i) to reconcile different neutrino anomalies including the LSND result; (ii) to explain an existence of the large mixing in the leptonic sector (in contrast with quark sector). Large mixing implied by the atmospheric neutrino data can be the mixing of  $\nu_\mu$

with sterile neutrino. All flavor mixings can be small. There is another indirect connection related to the fact that large (maximal) mixing prefers degeneracy of mass (see sect. 5.6).

If the atmospheric neutrino problem is solved due to oscillations of  $\nu_\mu$  and  $\nu_\tau$  strongly mixed in degenerate states, then there is no way to solve the solar neutrino problem. For this one can introduce sterile neutrino which mixes with  $\nu_e$ .

### 5.5. Intermediate mass scale scenario

Intermediate mass scale scenario is characterized by neutrino mass hierarchy, small mixing, and the Majorana masses of the right handed neutrinos (in the context of the see-saw) at the intermediate mass scale:  $10^{10} - 10^{13}$  GeV. In addition, the light singlet fermion can be introduced to solve the atmospheric neutrino problem [16] (fig. 10). The neutrino masses equal

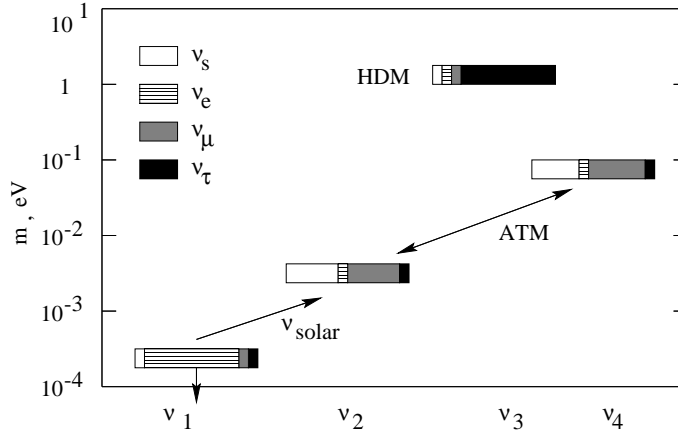


Fig. 10 Pattern of the neutrino mass and mixing in the intermediate mass scale scenario. Here white parts of boxes correspond to the sterile state.

$$m_4 = (0.3 - 3) \cdot 10^{-1} \text{eV}, \quad m_2 \sim 3 \times 10^{-3} \text{eV}, \quad m_3 \sim 1 \text{eV}, \quad m_1 \ll m_2. \quad (63)$$

In this scheme  $\nu_s$  and  $\nu_\mu$  are strongly mixed in the  $\nu_2$  and  $\nu_4$  eigenstates, so that  $\nu_\mu \leftrightarrow \nu_s$  oscillations solve the atmospheric neutrino problem;  $\nu_e \rightarrow \nu_\mu, \nu_s$  resonance conversion explains the solar neutrino data, and  $\nu_3$  can supply significant amount of the HDM.

The level crossing pattern (fig. 11) can be constructed in the following way. Let us introduce the eigenstates of strongly mixed subsystem  $\nu_\mu - \nu_s$ :  $\nu'_2$  and  $\nu'_4$ . At zero density they coincide with  $\nu_2$  and  $\nu_4$  up to small admixtures of the  $\nu_e$  and  $\nu_\tau$ . In the basis of the states  $(\nu_e, \nu'_2, \nu'_4, \nu_\tau)$  all the mixings are small.



As follows from fig. 11, there are four resonances in the neutrino channels and no level crossing in the antineutrino channels.

Let us consider the effects in supernova [16]. The transitions can be important for the nucleosynthesis of heavy elements due to  $r$ -processes. Above the  $\nu_e - \nu_\tau$  resonance at  $\rho > 10^8 (m_3/5eV)^2 \text{ g/cm}^3$  there is unchanged  $\nu_e$ -flux, whereas at  $\rho < 10^8 (m_3/5eV)^2 \text{ g/cm}^3$  the  $\nu_e$ -flux disappears thus producing conditions for neutron reach medium desired for  $r$ -processes. Indeed, in the  $\nu_e - \nu_\tau$  resonance,  $\nu_e$  are transformed to  $\nu_\tau$ , however inverse transition is absent:  $\nu_\tau$  are converted to  $\nu_s$  at about two times larger density and there is no inverse transition since there is no original flux of sterile neutrinos [33] (see however sect. 5.8). If all the

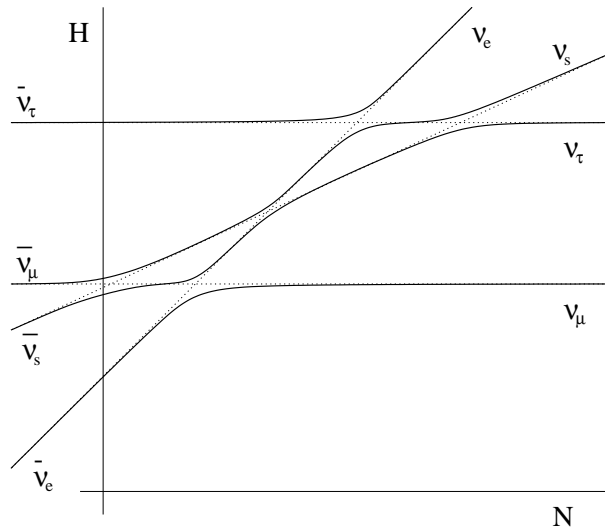


Fig. 11 The level crossing pattern for the intermediate mass scale scenario.

resonances are effective, the following transitions occur inside the star:

$$\nu_e \rightarrow \nu_\tau, \quad \nu_\mu \rightarrow \nu_e, \quad \nu_\tau \rightarrow \nu'_4 \rightarrow \nu_e \rightarrow \nu_2(\nu_\mu, \nu_s). \quad (64)$$

Thus at the Earth one expects: (i) disappearance of the  $\nu_e$  neutronization peak (appearance of the peak in non-electron neutrinos); (ii) the electron neutrinos with the hard spectrum (of original  $\nu_\mu$ ); (iii) tau neutrinos with soft spectrum (corresponding initial  $\nu_e$ ).

If resonances  $\nu_e - \nu_2$  and  $\nu_e - \nu_4$  (at low densities) are inefficient, the transitions proceed as:

$$\nu_e \rightarrow \nu_\tau, \quad \nu_\mu \rightarrow \nu_2(\nu_\mu, \nu_s), \quad \nu_\tau \rightarrow \nu_e \rightarrow \nu_4(\nu_\mu, \nu_s). \quad (65)$$

Thus, the neutronization peak changes the flavor, the flux of  $\nu_e$  in the cooling stage is strongly suppressed. Non-electron neutrinos will have soft component.

If  $\nu_e - \nu_\tau$  resonance is inefficient (because of smallness of  $U_{e3}$ ), the following transitions occur:

$$\nu_e \rightarrow \nu_4(\nu_\mu, \nu_s), \quad \nu_\mu \rightarrow \nu_e, \quad \nu_\tau \rightarrow \nu_2(\nu_\mu, \nu_s). \quad (66)$$

In this case the  $\nu_e$ -flux is unchanged in whole region of  $r$ -processes. At the detector, however,  $\nu_e$  will have a hard spectrum. The non-electron neutrino spectrum will have both hard and soft components.

### 5.6. Scheme with two degenerate neutrinos

Maximal mixing prefers strong mass degeneracy. Therefore the atmospheric neutrino result [34] can be considered as an indication that  $\nu_\mu$  and  $\nu_\tau$  are strongly mixed in the two heavy almost degenerate neutrino states:  $\Delta m \ll m_2 \approx m_3 \approx m_0$ . If  $m_0 \sim 1$  eV, these neutrinos can compose the  $2\nu$  HDM component in the Universe. In this case  $\Delta m \approx (2 - 5) \times 10^{-3}$  eV. The first neutrino composed, mainly, of  $\nu_e$  can be much lighter:  $m_1 \ll m_0$ , so that no observable signal in the double beta decay is expected. To explain the solar neutrino deficit one can introduce sterile neutrino which mixes with  $\nu_e$ . Then solar neutrinos can undergo the  $\nu_e \rightarrow \nu_s$  resonance conversion. The scheme (fig. 12) can also explain the LSND result if the admixture of the  $\nu_e$  in the heavy state is large enough  $U_{e3} \sim 2 \times 10^{-2}$  [37].

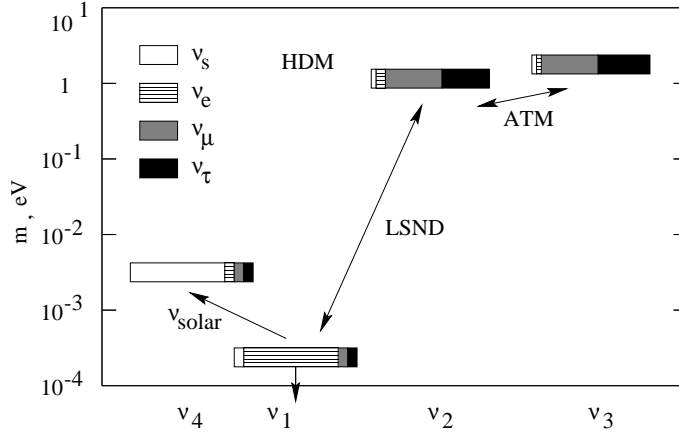


Fig. 12 The pattern of the neutrino mass and mixing in the scheme with two degenerate neutrinos and one sterile component.

With mixing required by the solar neutrino data and the LSND result both  $\nu_e - \nu_s$  and  $\nu_e - \nu_\tau$  resonances are in the adiabatic domain for supernovae. If all level crossings are adiabatic, then according to the level crossing scheme of fig. 12 one expects transitions:

$$\nu_e \rightarrow \nu'_3(\nu_\mu, \nu_\tau), \quad \nu'_2(\nu_\mu, \nu_\tau) \rightarrow \nu_s \rightarrow \nu_e, \quad \nu'_3(\nu_\mu, \nu_\tau) \rightarrow \nu_e \rightarrow \nu_s. \quad (67)$$

As the consequence, (i) the neutronization peak changes flavor; (ii) the electron neutrinos at the cooling stage have hard spectrum due to spectra interchange; (iii)  $\nu_s$  flux appears, and therefore total flux of the active neutrinos decreases; (iv) no modification of the  $\bar{\nu}_e$ -spectrum is expected.

Due to  $\nu_{ne} \rightarrow \nu_e$  conversion in the high density resonance the  $\nu_e$ - flux with hard spectrum appears in the outer part of the r-processes region. This will prevent from desired nucleosynthesis. The problem can be avoided if  $\nu_s$  admixture in the heaviest state is absent. Then, one of combinations  $(\nu_\mu, \nu_\tau)$ ,  $\nu'_3$  will transfer in to another combination of the same components  $\nu'_2$ , in turn  $\nu'_2$  is transformed into sterile neutrino, so that the  $\nu_e$ -flux in the outer part of the  $r$ -process region will be absent. The fluxes at the Earth will be similar to those in the previous

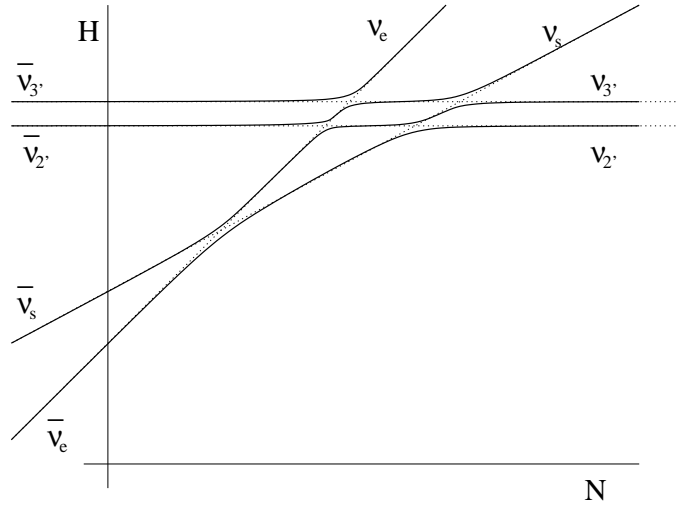


Fig. 13 The level crossing pattern in the scheme with two degenerate neutrinos and one sterile component.

case (67). The difference is that now there is no  $\nu_s$  flux at the exit, and the total flux of the active neutrinos is unchanged.

### 5.7. Grand Unification Scenario

The see-saw mechanism based on the Grand Unification leads to the mass of the heaviest neutrino ( $\approx \nu_\tau$ ) in the range  $(2 - 3) \cdot 10^{-3}$  eV, and hence, to a solution of the solar neutrino problem through the  $\nu_e \rightarrow \nu_\tau$  conversion. An existence of the light singlet fermion,  $\nu_s$ , which mixes predominantly with muon neutrino through the mixing mass  $m_{\mu s} \sim O(1)$  eV allows one [35] (i) to solve the atmospheric neutrino problem via the  $\nu_\mu \leftrightarrow \nu_s$  oscillations, (ii) to explain the LSND result and (iii) to get two component hot dark matter in the Universe (fig. 14). Similar scheme has been suggested previously in another context [36].

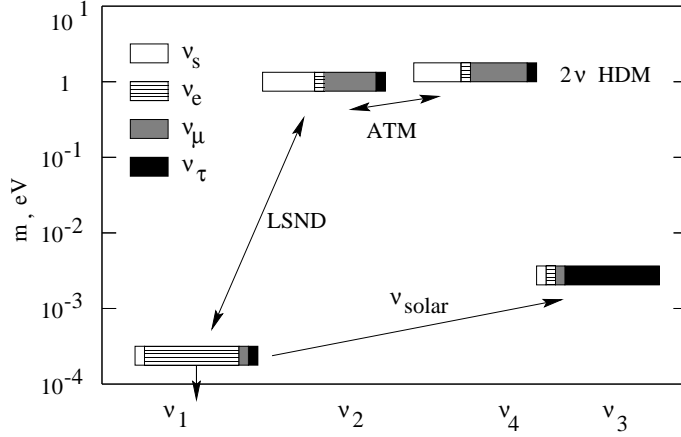


Fig. 14 The pattern of the neutrino mass and mixing in the Grand Unification scenario.

The level crossing pattern can be found in the following way (fig. 15). One diagonalizes first the strongly mixed heavy sub-system  $\nu_\mu$  and  $\nu_s$ . This gives the levels  $\nu'_{2m}, \nu'_{4m}$ . Then using smallness of all other mixings one gets the level crossings (resonances):  $\nu_e - \nu'_{4m}, \nu_e - \nu'_{2m}$  at large densities, and  $\nu_e - \nu_\tau$  crossing at small density. There is no level crossing in the antineutrino channels.

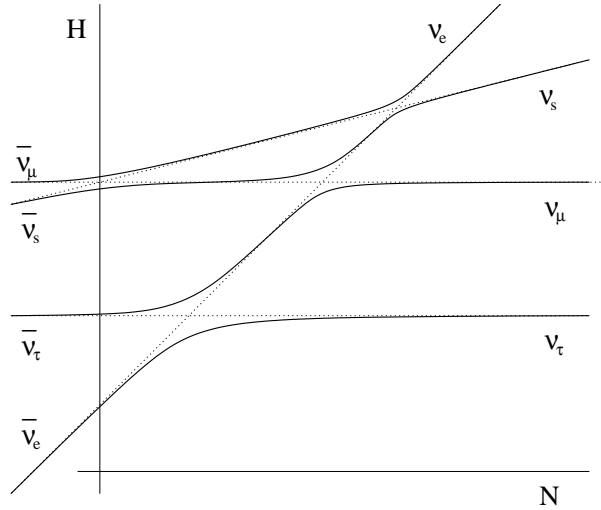


Fig. 15 The level crossing pattern in the Grand Unification scenario.

If the adiabaticity condition is fulfilled in all the resonances, one predicts the following transitions:

$$\nu_e \rightarrow \nu'_{4m} \approx (\nu_\mu + \nu_s)/\sqrt{2}, \quad \nu_\mu \rightarrow \nu_e \rightarrow \nu_\tau, \quad \nu_\tau \rightarrow \nu_e. \quad (68)$$

Thus, one can observe the electron neutrinos with hard spectrum,  $\nu_\mu$ 's with the

soft spectrum and the flux of sterile neutrinos being about 1/12 of the total neutrino flux. Half of the  $\bar{\nu}_\mu$ -flux will be converted to the  $\nu_s$ -flux. The production of the heavy elements due to the  $r$  - processes in supernovae imply that transitions  $\nu_\tau \rightarrow \nu_e$ ,  $\nu_\mu \rightarrow \nu_e$  are suppressed in the inner parts of the star [28]. As follows from the level crossing scheme the appearance of  $\nu_e$  can be due to adiabatic transition  $\nu_\mu \rightarrow \nu_e$ . The problem can be solved if  $\Delta m^2 \approx m_{\mu s}^2 < (1 - 2) \text{ eV}^2$ , so that the transitions occur in the outer layers above the  $r$ -processes region.

### 5.8. Matter induced resonance conversion

Previous analysis of transitions was based on assumption that no sterile neutrino flux is produced in the central regions of a star. This may not be true if  $\nu_e - \nu_s$  mixing mass term is large enough. Indeed, the effective potential for  $\nu_e - \nu_s$  channel (18) equals zero at

$$n_n = 2n_e . \quad (69)$$

This condition is satisfied in the layer with significant neutronization with  $\rho \sim 10^{11} \text{ g/cm}^3$ . Since  $\Delta m^2/2E \ll \sqrt{2}G_F\rho/m_N$  in this layer, the resonance condition takes the form  $V_{es} \approx 0$  [38]. Moreover, this condition is satisfied both for neutrinos and antineutrinos. Thus, at  $V_{es} \approx 0$  the resonance conversions  $\nu_e \rightarrow \nu_s$  and  $\bar{\nu}_e \rightarrow \bar{\nu}_s$  occur.

Thus, the level crossing schemes of Figs. 11, 13, 15 should be completed by two more resonances at densities  $\rho \sim 10^{11} \text{ g/cm}^3$  in the neutrino and in antineutrino channels.

Efficiency of transition in resonances is determined by the adiabaticity condition which in turn depends on mixing. The condition can be rewritten as:

$$\sin^2 2\theta > \frac{2E}{\Delta m^2 r_V} , \quad (70)$$

where  $r_V \equiv V/dV/dr$  is the scale height of the change of the effective potential. For  $r_V \sim 10 \text{ km}$  and  $E \sim 10 \text{ MeV}$  we get

$$\sin^2 2\theta > 10^{-2} \left( \frac{1\text{eV}}{m} \right)^2 . \quad (71)$$

If  $\nu_s$  mixes only in the light states (*e.g.* to explain the solar neutrino deficit), then  $m \sim 3 \times 10^{-3} \text{ eV}$  and clearly the adiabaticity condition is not satisfied. The situation can be different, when there is some admixture of  $\nu_s$  in the heavy mass eigenstates with  $m > 1 \text{ eV}$ . For instance, in the Grand Unification scenario (fig. 14) the  $\nu_e$  admixture in  $\nu_2$  or  $\nu_4$  required by the LSND data is enough to satisfy the adiabaticity condition (71) and therefore to induce strong  $\nu_e \rightarrow \nu_s$  and

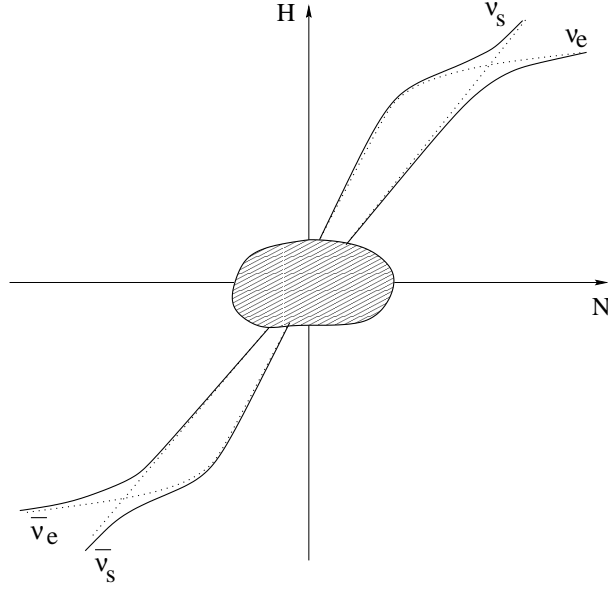


Fig. 16 The  $\nu_e - \nu_s$  and  $\bar{\nu}_e - \bar{\nu}_s$  level crossings in central parts of supernova. Dashed lines show the dependences of  $\nu_e$  and  $\nu_s$  energies on the total density. The shadowed region corresponds to the level crossing patterns shown in figs. 11, 13, 15.

$\bar{\nu}_e \rightarrow \bar{\nu}_s$  transitions in central parts of the star. Both transitions have practically the same efficiency.

Notice that  $\bar{\nu}_e \rightarrow \bar{\nu}_s$  transition leads to disappearance of the  $\bar{\nu}_e$  signal which is crucial for the present searches of the  $\nu$ -bursts from supernovae. The observation of  $\bar{\nu}_e$  signal from SN87A gives the bound on  $\bar{\nu}_e \rightarrow \bar{\nu}_s$  transition and therefore on mixing of  $\nu_e$  in the heavy state. At the same time, an efficiency of the transition depends on model of the star, and in particular, on its mass. For some class of stars, like SN87A, the transition can be less efficient leading to partial (weak) suppression of signal. For other cases the transition can be strong. This is clearly, important for  $\nu$ -burst detection.

Notice also that transitions  $\nu_e \rightarrow \nu_s$  and  $\bar{\nu}_e \rightarrow \bar{\nu}_s$  lead to disappearance of the  $\nu_e$ -flux in the inner part of the  $r$ -processes region and disappearance of the  $\bar{\nu}_e$ -flux in whole the region.

## 6. Conclusions

Variety of physical conditions, the effective density profiles and still possible neutrino mass spectra leads to a variety of possible neutrino conversion phenomena.

The picture of the neutrino transformations depends significantly on scheme

of neutrino mass and mixing. The medium effects are minimal in the case of strict bi-maximal mixing. In this case, matter can only suppress mixing in the  $\nu_e$ -channels of oscillations, and still the results are the same as in the case of averaged vacuum oscillations. In contrast, there is a richness of the matter effects in schemes with small mixing and especially in schemes with sterile neutrinos.

The study of supernova neutrinos will allow one to test whole spectrum of neutrino masses.

### Acknowledgement

I would like to thank H. Minakata and O. Yasuda for hospitality during my stay at TMU. The author is grateful to A. Dighe, H. Minakata and F. Vissani for fruitful discussions and comments.

### References

- [1] L. Wolfenstein, Phys. Rev. D17 (1978) 2369.
- [2] S. P. Mikheyev and A. Yu. Smirnov, Sov. J. Nucl. Phys. 42 (1985) 913.
- [3] H. Nunokawa, V. B. Semikoz, A. Yu. Smirnov, J. W. F. Valle, Nucl. Phys. B501 (1997) 17.
- [4] P. Langacker, J. P. Leveille, J. Sheiman, Phys. Rev. **D27** (1983) 1228.
- [5] V. Semikoz, Yad. Fiz **46** (1987) 1592 [Sov. J. Nucl. Phys. **46** (1987) 946]; J. C. D'Olivo, J. Nieves and P. B. Pal, Phys. Rev. **D40** (1989) 3679; S. Esposito and G. Capone, Z. Phys. **C70** (1996) 55.
- [6] P. Elmfors, D. Grasso and G. Raffelt, Nucl. Phys. **B479** (1996) 3.
- [7] V. Semikoz and J. W. F. Valle, Nucl. Phys. **B425** (1994) 651; erratum Nucl. Phys. **B485** (1997) 545.
- [8] J.C. D'Olivo and J. Nieves, Phys. Lett. **B383** (1996) 87.
- [9] A. Kusenko and G. Segre, Phys. Rev. Lett. **77** (1996) 4872.
- [10] D. Nötzold and G. Raffelt, Nucl. Phys. **B307** (1987) 924.
- [11] R. Foot, M.J. Thomson and R. R. Volkas, Phys. Rev. D **53**, 5349 (1996); X. Shi, Phys. Rev. **D54**, (1996) 2753; R. Foot and R.R. Volkas, Phys. Rev. **D55**, (1997) 5147.

- [12] S. P. Mikheyev and A. Yu. Smirnov, Proc. of the 6th Moriond Workshop on massive Neutrinos in Astrophysics and Particle Physics, Tignes, Savoie, France (eds. O. Fackler and J. Tran Thanh Van) p. 355 (1986); J. Bouchez *et al.*, Z. Phys. C **32** (1986) 499; V. K. Ermilova, V. A. Tsarev, V. A. Chechin, JETP Lett. **43** (1986) 453.
- [13] V. K. Ermilova, V. A. Tsarev and V. A. Chechin, Kr. Soob, Fiz. [Short Notices of the Lebedev Institute] **5**, 26 (1986).
- [14] E. Kh. Akhmedov, preprint IAE-4470/1, (1987); Yad. Fiz. **47**, 475 (1988) [Sov. J. Nucl. Phys. **47**, 301 (1988)].
- [15] P. I. Krastev and A. Yu. Smirnov, Phys. Lett. B **226**, 341 (1989).
- [16] Q. Y. Liu, A. Yu. Smirnov, Nucl. Phys. **B 524** (1998) 505.
- [17] Q. Y. Liu, S. P. Mikheyev, A. Yu. Smirnov, hep-ph/9803415.
- [18] S. T. Petcov, Phys. Lett. **B434** (1998) 321.
- [19] E. Kh. Akhmedov, hep-ph/9805272.
- [20] P. I. Krastev, A. Yu. Smirnov, Mod. Phys. Lett. **A6** (1991) 1001.
- [21] see *e.g.* A. De Rujula et al., Nucl. Phys. **B168** (1980) 54; V. Barger and K. Whisnant, Phys. Lett. **B209** (1988) 365; S. M. Bilenky et al., Phys. Lett. **B276** (1992) 223.
- [22] see *e.g.* C-S. Lim, BNL-39675 (1987).
- [23] J. Pantaleone, Phys. Rev. D **49** (1994) R2152.
- [24] C. Giunti, C. W. Kim, and M. Monteno, hep-ph/9709439.
- [25] G. L. Fogli, E. Lisi, A. Marone, D. Montanino, Phys. Lett. **B425** (1998) 341.
- [26] A. E. Chudakov, O. G. Ryazhskaya, G. T. Zatsepin, In Denver 1973, Cosmic Ray Conference, Vol. 3, (1973), 2007, S. P. Mikheev, A. Yu. Smirnov, Sov. Phys. JETP **64** (1986) 4, Zh. Eksp. Teor. Fiz. **91** (1986) 7; JETP Lett. **46** (1987) 10.
- [27] G. M. Fuller et al., Astrophys. J., **322** (1987) 795; T. K. Kuo, J. Pantaleone, Phys. Rev. **D37** (1988) 298; H. Nunokawa et al., Phys. Rev. **D54** (1996) 4356; H. Nunokawa, A. Rossi, J.W.F. Valle, Nucl. Phys. **B482** (1996) 481; B. Jegerlehner, F. Neubig, G. Raffelt, Phys. Rev. **D54** (1996) 1194; H. Nunokawa, J.T. Peltoniemi, A. Rossi, J.W.F. Valle Phys. Rev. **D56** (1997) 1704.



- [28] Y.-Z. Qian, G. M. Fuller, G. J. Mathews, R. Mayle, J. R. Wilson, S.E. Woosley, Phys. Rev. Lett. **71** (1993) 1965; W. C. Haxton, K. Langanke, Y.Z. Qian, P. Vogel, Phys. Rev. Lett. **78** (1997) 2694.
- [29] A. Yu. Smirnov, D. N. Spergel, J. N. Bahcall, Phys. Rev. **D49** (1994) 1389.
- [30] A. Dighe and A. Yu. Smirnov, in preparation.
- [31] see for recent discussion H. Minakata and O. Yasuda, Phys. Rev. **D56** (1997) 1692; Nucl. Phys. **B523** (1998) 597.
- [32] see e.g. F. Vissani, hep-ph/9708483; V. Barger, S. Pakvasa, T. Weiler and K. Whisnant, hep-ph/9806387, A. Baltz, A. S. Goldhaber and M. Goldhaber, hep-ph/9806540, H. Georgi and S. L. Glashow, hep-ph/9808293.
- [33] J. T. Peltoniemi, hep-ph/9506228.
- [34] T. Kajita, Talk presented at Neutrino '98, Y. Fukuda *et al.*, hep-ex/9807003.
- [35] A. S. Joshipura, A. Yu. Smirnov, hep-ph/9806376.
- [36] J. T. Peltoniemi, D. Tomasini and J. W. F. Valle, Phys. Lett. **B298** (1993); E. J. Chun, C. W. Kim and U. W. Lee, hep-ph/9802209.
- [37] J.T. Peltoniemi and J.W.F. Valle, Nucl. Phys. B **406**,(1993) 409; D.O. Caldwell and R.N. Mohapatra, Phys. Rev.**D48**, (1993) 3259; Z. Berezhiani and R.N. Mohapatra, Phys. Rev. **D52**, 6607 (1995); E. Ma and P. Roy, Phys. Rev. **B52**, R4780 (1995); E.J. Chun *et al.*, Phys. Lett. **B357**, (1995) 608; R. Foot and R.R. Volkas, Phys. Rev. **D52**, (1995) 6595; J.J. Gomez-Cadenas and M.C. Gonzalez-Garcia, Z. Phys. C **71**, (1996) 443; S.M. Bilenkii, C. Giunti, W. Grimus Eur. Phys. J. **C1** (1998) 247; E. Ma, Mod. Phys. Lett. A **11**, (1996) 1893; S. Goswami, Phys. Rev. **D55**, (1997) 2931; A. Yu. Smirnov and M. Tanimoto, Phys. Rev. **D55**, (1997) 1665; V. Barger, T.J. Weiler and K. Whisnant, hep-ph/9712495.
- [38] M.B. Voloshin, Phys. Lett. **B209** (1988) 360.